

# Definition of an electronic profile of compounds with inhibitory activity against hematin aggregation in malaria parasite<sup>☆</sup>

César Portela,<sup>a</sup> Carlos M. M. Afonso,<sup>a</sup> Madalena M. M. Pinto<sup>a</sup> and Maria João Ramos<sup>b,\*</sup>

<sup>a</sup>*Centro de Estudos de Química Orgânica, Fitoquímica e Farmacologia da Universidade do Porto, Faculdade de Farmácia, Rua Aníbal Cunha, 164 4050-047 Porto, Portugal*

<sup>b</sup>*REQUIMTE, Departamento de Química, Faculdade de Ciências, Universidade do Porto, Rua do Campo Alegre, 687 4169-007 Porto, Portugal*

Received 23 January 2004; accepted 26 March 2004  
Available online 6 May 2004

**Abstract**—Malaria is one of the most important parasitic diseases, affecting almost half of the world and posing a threat to the other half. Xanthone derivatives can behave as antimalarial drugs in the same mechanistic way as chloroquine and other related quinolines. This action is due to the inhibition of the detoxification pathway of the parasite, responsible for the production of hemozoin. We report a study of the electronic properties of the xanthonic and quinolinic compounds based on DFT calculations, in order to determine a pattern that could be applied to the development of new potentially active antimalarial molecules. As a result, a new interpretation of structure–activity relationship of the quinoline antimalarial drugs, and of the active hydroxylated xanthenes is proposed here. We conclude that electronic features rather than steric factors control primarily the inhibitory activity of the studied compounds against hematin aggregation, concurring to a potential antimalarial activity.

© 2004 Elsevier Ltd. All rights reserved.

## 1. Introduction

Malaria is a public health problem in more than 90 countries, which are inhabited by a total of 2400 million people—40% of the population of our planet. It has a prevalence of the order of 300–500 million clinical cases, killing over 1 million people each year. The great majority of deaths is among children, with one dying every 30 seconds.<sup>1–3</sup> Due to the lack of professional help, therapy is often incomplete and performed with irrational methods, speeding up the development and spreading of resistance to drugs currently in use.<sup>4–8</sup> The search for new antimalarial agents, which constitute an alternative to the currently used drugs, is imperative.

The malaria parasite has a limited capacity for *de novo* amino acid synthesis, and its survival is dependant on hemoglobin proteolysis. The amino acids derived from globin hydrolysis are incorporated into parasite proteins

and appear to be available also for energy metabolism. This digestion of hemoglobin releases the heme moiety, which oxidizes to hematin, also known as ferriprotoporphyrin IX (Fig. 1).<sup>9</sup> Free hematin can damage cellular metabolism by inhibition of enzymes, the peroxidation of membranes, and the production of

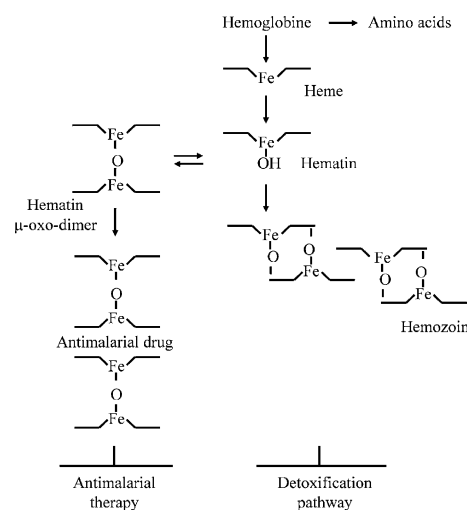


**Figure 1.** Schematic representation of heme detoxification pathway of the malaria parasite—target for the antimalarial action.

**Keywords:** Antimalarial; Hematin; Hemozoin; Malaria.

<sup>☆</sup>Supplementary data associated with this article can be found, in the online version, at [doi:10.1016/j.bmc.2004.03.060](https://doi.org/10.1016/j.bmc.2004.03.060)

\*Corresponding author. Tel.: +351-22-6082806; fax: +351-22-60829-59; e-mail address: [mjramos@fc.up.pt](mailto:mjramos@fc.up.pt)

oxidative free radicals in the acidic environment of the digestive vacuole.<sup>9</sup> Lacking the heme oxygenase that vertebrates use for heme catabolism, plasmodial species sequester this toxic by-product into a chemically inert crystal.<sup>9</sup> The product formed, hemozoin, is an aggregate of several units of hematin linked by carboxylate–iron(III) and carboxylate–carboxylate coordinated bonds.<sup>10–12</sup> The aggregation process is a mechanism of detoxification that can be used as a target for antimalarial therapy.<sup>13–15</sup> Thus, several antimalarial compounds work by stabilizing a derivative form of hematin, a  $\mu$ -oxo-dimer, avoiding the association of these units in the hematin aggregation process (Fig. 2, Table 1).<sup>16–18</sup> The hematin  $\mu$ -oxo-dimer is a complex of two molecules of hematin connected by an oxygen bridge between the two iron atoms.<sup>12</sup>

The death of the parasite arises as a consequence of the toxicity of the free hematin.<sup>19–24</sup> Considerable data now support the hypothesis that antimalarial quinolines inhibit parasite growth by binding to hematin<sup>25–29</sup> preventing its aggregation into the form of hemozoin.<sup>13,30,31</sup> This was the mechanism of action established for drugs as chloroquine, amodiaquine, mepacrine among other 4-aminoquinolines (Fig. 2, Table 1).<sup>28,29,32–38</sup>

Drugs like quinolinemethanol mefloquine or phenanthrenemethanol halofantrine, albeit not having a clearly

**Table 1.** Inhibitory activity against the hematin aggregation process for antimalarial compounds used in therapy<sup>32</sup>

Compound	IC <sub>50</sub> ( $\mu$ M) for hematin aggregation
Chloroquine	24.4
Amodiaquine	15.1
Amopyroquine	29.5
Tebuquine	52.7
Pyronaridine	64.4
Mepacrine	41.0
Mefloquine	46.9
Halofantrine	184.5

defined pharmacological mechanism, also present the ability of inhibiting this aggregation phenomenon (Fig. 2, Table 1).<sup>28,29,33–35</sup> As the side chains of 4-aminoquinolines are not involved in hematin association or inhibition of the hematin aggregation phenomenon, the calculations in this work were performed only on the aromatic moieties, as explained in Figure 3.<sup>39–45</sup>

Some compounds, although structurally similar, do not show inhibitory activity against hematin aggregation (compounds 2 and 3).<sup>39–41</sup> This lack of activity is justified in this study with the demonstration of their different electronic properties. Thus, compounds 2 and 3 (Fig. 3) were used to determine the electronic behavior provided by the chlorine atom and its position in the aromatic nucleus.

Other studies concerning hydroxylated xanthenes (Fig. 4) have shown that these compounds present antimalarial activity, in *in vitro* assays (Table 2).<sup>46–49</sup> Xanthenes (9H-xanthen-9-ones) are heterocyclic compounds with the dibenzo- $\gamma$ -pyrone framework.<sup>50,51</sup> Although structurally different, xanthonic structures have the capability of inhibiting hematin aggregation, just as 4-aminoquinolines, quinolinemethanols, and phenanthrenemethanols. This fact has been stated as their pharmacological mechanism of antimalarial action.<sup>48,49</sup>

The present study is an assessment of structural and electronic properties of the 4-aminoquinolines, quino-

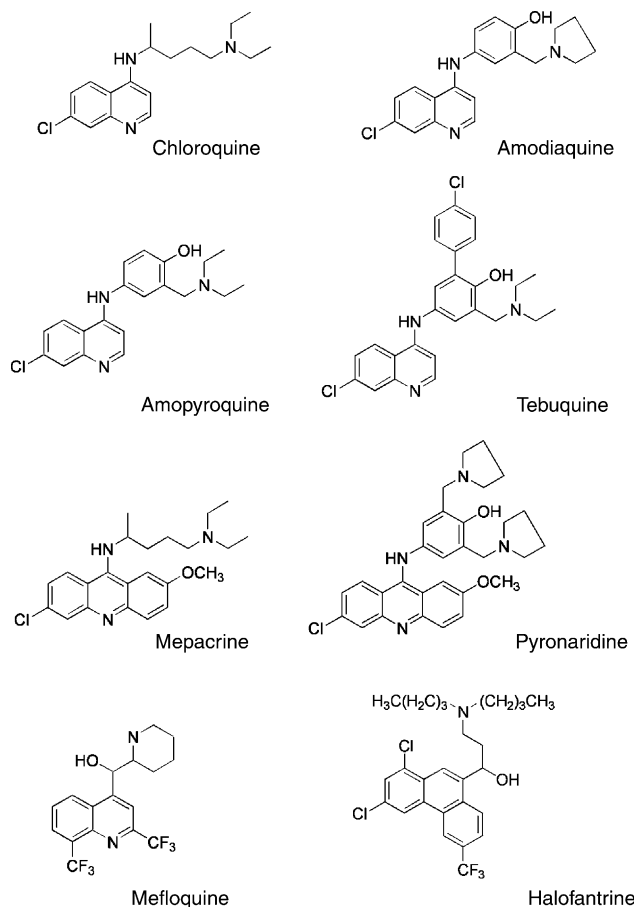


**Figure 2.** Antimalarial compounds with inhibitory activity over hematin aggregation.

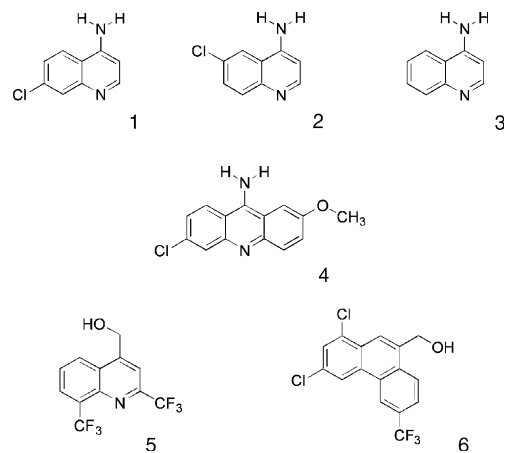


**Figure 3.** Aromatic moieties: (1) Chloroquine, amodiaquine, amopyroquine, and tebuquine; (2) 4-amino-6-chloro-quinoline; (3) 4-amino-quinoline; (4) pyronaridine and mepacrine; (5) mefloquine; (6) halofantrine.

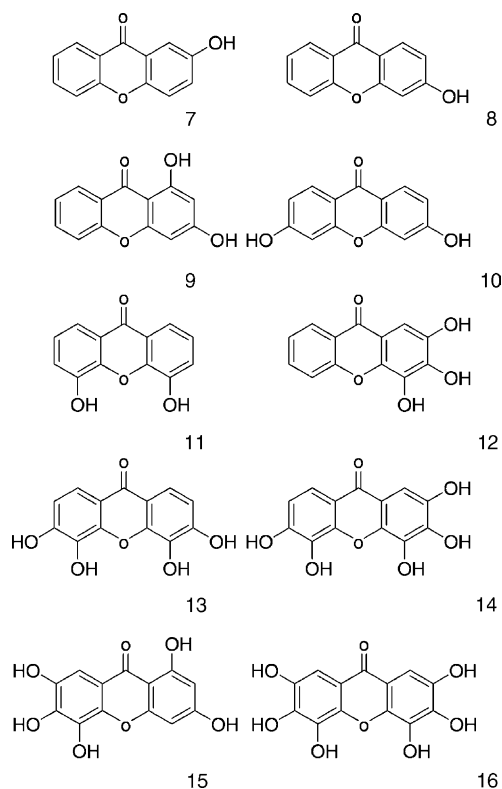


**Figure 4.** Xanthone derivatives: (7) 2-hydroxyxanthone; (8) 3-hydroxyxanthone; (9) 1,3-dihydroxyxanthone; (10) 3,6-dihydroxyxanthone; (11) 4,5-dihydroxyxanthone; (12) 2,3,4-trihydroxyxanthone; (13) 3,4,5,6-tetrahydroxyxanthone; (14) 2,3,4,5,6-pentahydroxyxanthone; (15) 1,3,5,6,7-pentahydroxyxanthone; (16) 2,3,4,5,6,7-hexahydroxyxanthone.

**Table 2.** Inhibitory activity against the hematin aggregation process for xanthone derivatives<sup>45</sup>

Compound	IC <sub>50</sub> (μM) for hematin aggregation
7	>1000
8	>1000
9	>1000
10	>500
11	14
12	17
13	2, 5
14	1, 2
15	9
16	1, 4

linemethanols, and phenantrenemethanols aromatic moieties (Fig. 3), and of xanthone derivatives (Fig. 4).

A study over the electronic properties of the receptor was also performed to determine how drug–receptor interactions could occur.

The computational procedure was carried out using density functional theory, allowing a better determination of the electronic properties of the studied compounds. This method conjugates the possibility of introducing the concept of electronic correlation in the calculations, with a computational effort similar to the Hartree–Fock methods.

The data obtained allowed the establishment of a relationship between the active compounds, providing the definition of an electronic profile pattern. This electronic profile points to a successful interaction between the active compounds and hematin, leading to stabilization and avoiding a further aggregation into hemozoin.

This established profile should be an important tool for the design of new molecules with antimalarial activity.

## 2. Results and discussion

Values of energy for the aromatic moieties and xanthone derivatives are given in Table 3, as well as a qualitative evaluation of inhibitory activity over the hematin aggregation process.

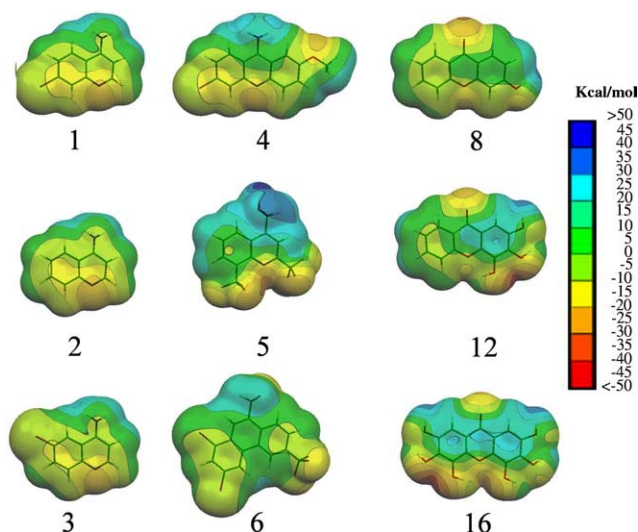
MEPs superimposed onto total electron density and three-dimensional electrostatic potential isosurfaces at  $-10$  and  $-5$  kcal/mol are presented in Figures 5 and 6, for compounds 1–6, 8, 12, and 16 (schematic representations can be viewed in Figs. 3 and 4). All calculations have been carried out in vacuo. The three-dimensional MEP maps superimposed onto total electron density account for the interpretation of short-range interactions between molecules. At each point of the map, the electrostatic potential expresses the value of the electrostatic energy of interaction with a unitary positive charge. This representation helps to interpret how interactions between a drug and its receptor can occur.

Figure 5 shows the three-dimensional MEP maps superimposed onto total electron density for structures 1–6 (schematic structures in Fig. 3). These data reveal that the center of the most negative potential in the aromatic moieties of the active compounds lies in the

**Table 3.** Values of energy for the aromatic moieties and xanthone derivatives

Compound	Inhibition over hematin aggregation	Energy (kJ/mol)
1	+	–2407, 2745
2	–	–1200, 5402
3	–	–2407, 209
4	+	–3111, 3305
5	+	–3125, 7023
6	+	–5015, 4547
7	–	–1905, 7992
8	–	–1905, 8106
9	–	–2103, 2693
10	–	–2103, 2953
11	+	–2103, 2727
12	+	–2300, 7558
13	+	–2498, 2263
14	+	–2695, 709
15	+	–2695, 7019
16	+	–2893, 1926

Qualitative evaluation of inhibitory activity over the hematin aggregation process.



**Figure 5.** MEPs superimposed onto total electron density at a value of  $0.0002 \text{ e/au}^3$  for compounds 1–6 (Fig. 3) and 8, 12, and 16 (Fig. 4).

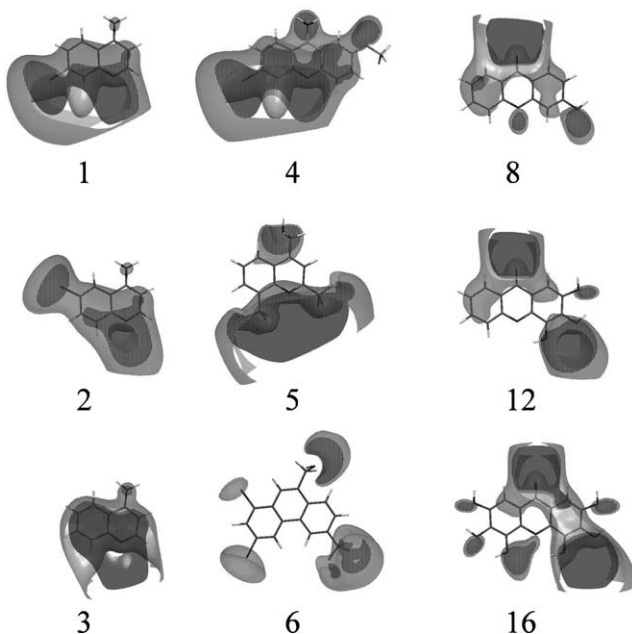


**Figure 6.** Three-dimensional electrostatic potential isosurfaces at  $-10 \text{ kcal/mol}$  (dark grey) and  $-5 \text{ kcal/mol}$  (light grey) for compounds 1–6 (Fig. 3) and 8, 12, and 16 (Fig. 4).

vicinity of the quinoline nitrogen atom, being this negativity reinforced by the electron withdrawing groups ( $-\text{Cl}$ ,  $-\text{CF}_3$ ) present at this particular side of the molecule. As for the center of the most positive potential, this lies in the amino group (compounds 1–4) or in the hydroxyl oxygen (compounds 5 and 6). The quinoline ring presents a value of electrostatic potential superior to  $-5 \text{ kcal/mol}$ , defining a susceptibility to nucleophilic attack. A relationship between electronic behavior and antimalarial activity has been previously determined,<sup>33,44,45,52,53</sup> stating that the quinoline ring plane is more susceptible to nucleophilic attack in compounds with potent antimalarial activity, whereas sus-

ceptibility for electrophilic attack on the quinoline ring reduces activity. This is demonstrated by the absence of a strong negative potential located on the aromatic rings of the compounds exhibiting an inhibitory activity over the hematin aggregation process.

Also depicted in Figure 5 are the three-dimensional MEP maps superimposed onto total electron density for compounds 8, 12, and 16 (schematic structures in Fig. 4). Xanthenes show a positive potential placed at the center of the rings, being the negative potential located in the carbonyl and hydroxyl oxygens. The compounds that show a better antimalarial activity, present higher positive values of potential connected with the aromatic rings. This might mean that the susceptibility to nucleophilic attacks on the rings of this group of compounds is of importance for the association with hematin, and the development of their antimalarial action.

The three-dimensional MEP isosurfaces can account for the interpretation of long-range interactions. This knowledge might allow the determination of an electrostatic pattern between the compounds that attach to the hematin  $\mu$ -oxo-dimer, stabilizing it. These isosurfaces have been determined at values of  $-10$  and  $-5 \text{ kcal/mol}$  for compounds 1–6, 8, 12, 16 (Fig. 6).

The three-dimensional MEP isosurfaces of the active 4-aminoquinoline derivatives (structures 1 and 4, Fig. 6) show a negative potential region extended from the quinoline ring nitrogen atom to the chlorine present in the adjacent ring. This region can be divided in two zones, one placed around the chlorine atom and the other containing the quinoline ring nitrogen. This observation shows the influence of the chlorine atom and its position. The inactive quinolines 2 and 3 show very different distributions of electrostatic potential (Fig. 2). This observation confirms the influence of the chlorine atom and the importance of its position.<sup>39–41</sup> The importance of the chlorine in the inhibition of the aggregation of hematin to form hemozoin has been previously referred, determining that its presence in position 6 (structure 2, Fig. 3), or its absence on the quinoline ring system (structure 3, Fig. 3) concurred to inactivity. The presence of the chlorine atom in position 7 (structure 1, Fig. 3) concurred to the higher activity.<sup>39–41</sup> Thus, activity could be due to the electronic properties shown by these molecules as a consequence of the electron withdrawing nature of their substituents, together with their relative position. This electronic profile would be responsible for their action, allowing a connection to the hematin  $\mu$ -oxo-dimer, stabilizing its structure and avoiding the subsequent aggregation into hemozoin.

The mefloquine aromatic moiety (structure 5, Fig. 6) shows a large negative potential region corresponding to the quinoline ring nitrogen atom and the trifluoromethyl substituents zone. This bulk of negative potential seems to be essential for activity in this compound.<sup>44,45,52</sup> The removal and replacement of these substituents, altering this electronic profile, leads to a decrease in potency.<sup>52</sup>

A common electronic behavior can be established based on this information:

- the absence of a strong negative potential placed over at least a part of the aromatic rings;
- the existence of two bulks of negative potential placed on two points or a negative potential extending over these two points.

As for the halofantrine aromatic moiety (structure 6, Fig. 6), although it presents smaller surfaces of negative potential at the measured values, they are placed in positions that correlate with the pattern previously referred. The smaller surfaces could determine a smaller inhibition capability.

The calculations presented here were carried out in order to establish a parallel between this type of compounds and the hydroxylated xanthonic structures with the same activity present in the second group, allowing the definition of a pattern between the electronic profiles of the active compounds.

The MEP isosurfaces of compounds 7–16 show two distinct electronic profiles. The profile corresponding to the active compounds (structures 11–16, Fig. 4, Table 2) presents two bulks of negative potential. One of them is placed at the carbonyl oxygen, with the other located in the area corresponding to the hydroxyl oxygen in position 4. The proximity of other hydroxyl groups favors activity with the decrease of the negative potential in that area of the molecule (represented by compounds 12 and 16, Fig. 6).

Taking into consideration the fact that the compounds presenting activity interact with hematin, inhibiting hematin aggregation, a common electronic profile should exist between them. The superimposing of active molecules 1, 4, 5, 6, and 11–16, together with their electrostatic potential isosurfaces, reinforces the idea that an electronic profile pattern exists (Fig. 7). In fact:

- The bulk of negative potential in the carbonyl oxygen could display the same function as the negative potential near the quinoline ring nitrogen atom in 4-aminoquinolines aromatic moieties 1 and 4 or the trifluoromethyl groups in the quinolinemethanols (5) and phenantrenemethanols (6).
- The negative potential bulk corresponding to the hydroxyl groups in active xanthone derivatives (12–18) could correspond to the negative potential originated by the chlorine and trifluoromethyl groups.

Mefloquine aromatic moiety (5) exhibits an electrostatic surface that covers all the area around these two points, as already pointed out.

Based on these observations, we can propose a group of characteristics that would be implied in the achievement of activity:

- the presence of two bulks of negative potential placed at a distance of 9.6–12.1 Å from each other (Fig. 8);

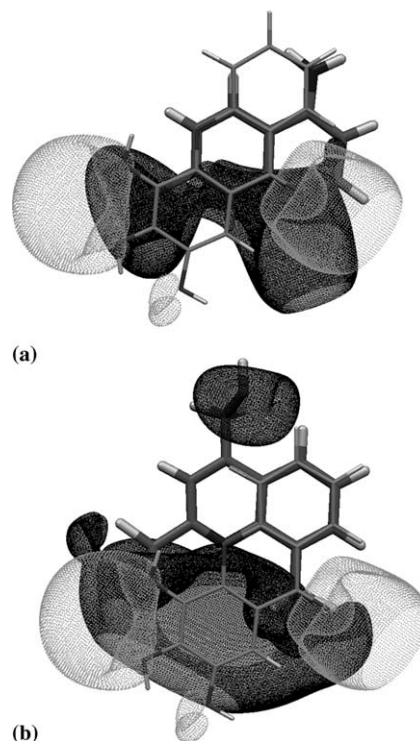


**Figure 7.** Correspondence between the electrostatic potential isosurfaces between different compounds at  $-10$  kcal/mol: (a) aromatic moiety (structure 1, Fig. 3) of chloroquine (dark grey and black) and 2,3,4-trihydroxyxanthone (light grey); (b) aromatic moiety (structure 5, Fig. 3) of mefloquine (dark grey and black) and 2,3,4-trihydroxyxanthone (light grey).

- the presence of a null or positive potential, over at least a part of the aromatic rings, placed as a third point of the triangle defined together with the two points referred above (Fig. 8).

The three-dimensional MEP map superimposed onto total electron density of the hematin  $\mu$ -oxo-dimer

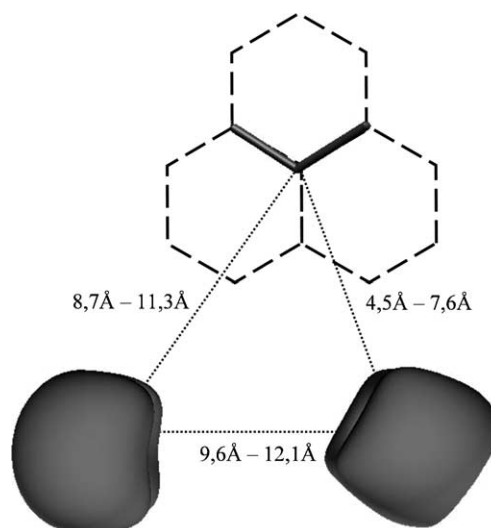


**Figure 8.** Parameters of active compounds involved in the definition of an inhibitory activity over the hematin aggregation process.



exhibits a profile complementary to the one corresponding to the active compounds, with values of potential ranging from  $-50$  to  $30$  kcal/mol (Fig. 9). The most negative potential is located on the position occupied by the iron atoms and the tetrapyrrol system, with the most positive potential found at the propionic groups (see Fig. 9). The electrostatic potential isosurfaces at values of  $-10$  kcal/mol shows a large surface centered on the dimer (Fig. 10), also corresponding to the iron, oxygen bridge and pyrrolic nitrogen atoms system. The carboxylic groups present a negative potential located on the oxygen atoms, with a positive potential placed on the carbon and the hydrogen atoms.

Observing the distribution of electrostatic potential in this receptor, we can define a triangle pattern composed of two points of positive potential and one point of negative potential (Fig. 11). The active drugs present an opposite profile, with a triangle pattern composed of two points of negative potential and one point of null to positive potential.

The antimalarial compounds can therefore act by stabilizing the dimer due to the long range interactions determined by their complementary electrostatic profiles, avoiding a further aggregation of these units to

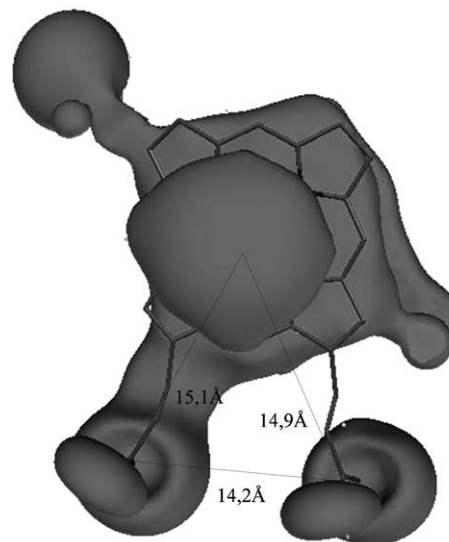


**Figure 11.** Parameters of the receptor involved in the interaction with active compounds presenting an inhibitory activity over the hematin aggregation process.

form hemozoin. The positive potential of the aromatic ring of the active compounds would interact with the

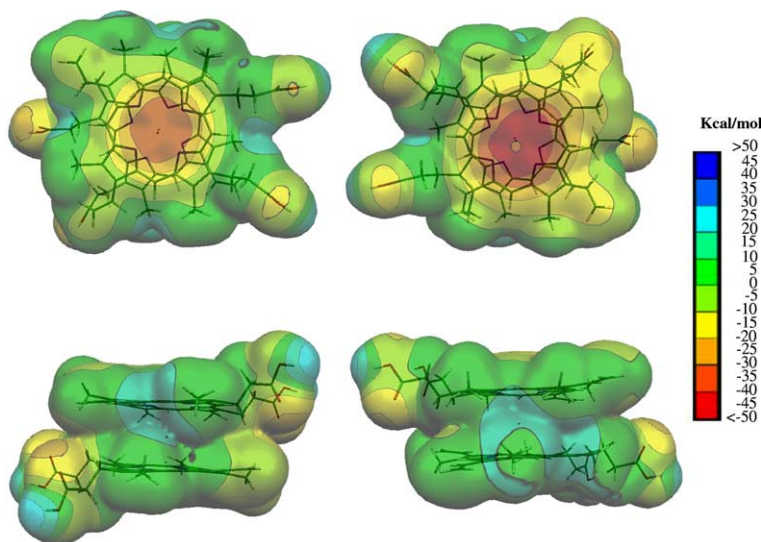


**Figure 9.** MEPs superimposed onto total electron density at a value of  $0.0002 \text{ e/au}^3$  for the hematin  $\mu$ -oxo-dimer.

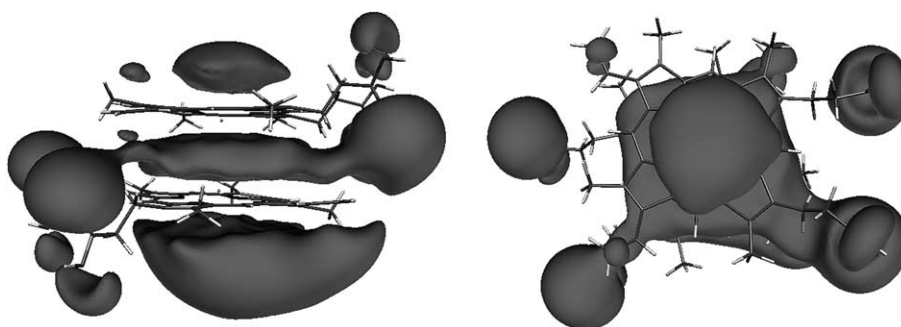


**Figure 10.** Three-dimensional electrostatic potential isosurface at  $-10$  kcal/mol for the hematin  $\mu$ -oxo-dimer.

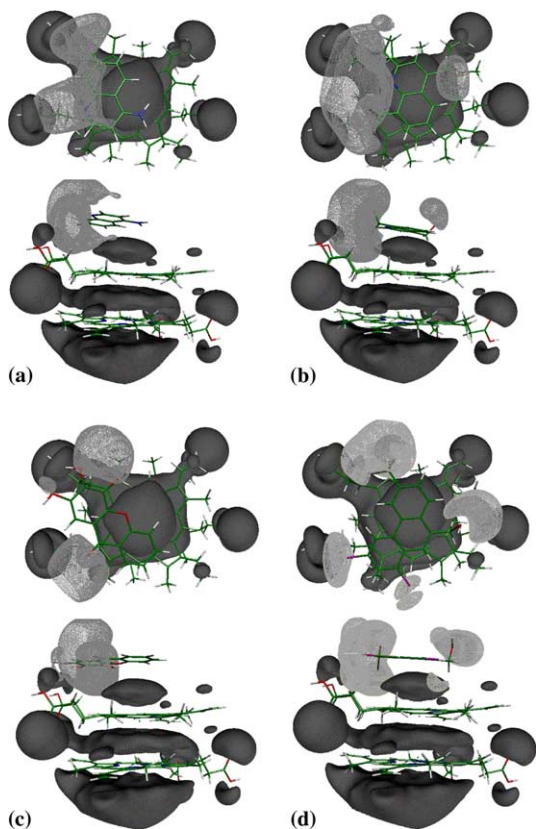


**Figure 12.** Complementarity of three-dimensional electrostatic potential isosurfaces at  $-10$  kcal/mol between the hematin  $\mu$ -oxo-dimer and: (13a) aromatic moiety of chloroquine; (13b) aromatic moiety of mefloquine; (13c) 2,3,4-trihydroxyxanthone; (13d) aromatic moiety of halofantrine.

negative potential on the center of the dimer. The regions of negative potential for the same compounds would stabilize the positive potential peripheral to the tetrapyrrol system of the hematin complex (Fig. 12).

### 3. Conclusion

The investigation of the electronic features of the 4-aminoquinolines, quinolinemethanols, phenantrene-methanols and of xanthone derivatives has resulted in the following profile for the exhibition of an inhibitory activity over the hematin aggregation process:

- the existence of two points of large negative potential, or the existence of one large broad lateral negative potential extending between and over these two points;
- the presence of a null or positive potential, above and below the aromatic rings or part of them, placed as a third point of the triangle defined together with the two points referred above.

The areas of negative potential of the active compounds are likely to be responsible for the interactions with the

peripheral area of the hematin dimer, presenting positive potential. The positive potential positioned on the aromatic rings of the active compounds can be involved in the interaction with the iron-pyrroles environment in the  $\mu$ -oxo-dimer.

We conclude that electronic features rather than steric factors seem to control primarily the inhibitory activity against hematin aggregation, concurring to a potential antimalarial activity.

The design of new xanthone derivatives with antimalarial activity based on the established profile, as well as the structure–activity relationships, is underway.

### 4. Computational procedure

All calculations were performed with the GAUSSIAN 98 package.<sup>54</sup> Geometry optimizations and energy calculations were performed on each compound at the ab initio quantum mechanical level by using density functional theory (DFT) with the Becke3-Lee-Yang-Parr (B3LYP) functional, and the 6-31G(d) basis set. Initially, in fact, calculations were performed using the 3-21G basis set for the optimization step, followed by a single point calculation at the 6-31G(d) level; however, as the results were different from those obtained with the method referred above, we have opted to use the more precise basis set 6-31G(d).

The geometry optimization and energy calculations of the  $\mu$ -oxo-dimer of hematin were performed using the CHARMM force field present in the Quanta package, followed by a single point calculation using DFT with the B3LYP functional and the 6-31G(d) basis set. Both hemozoin and the  $\mu$ -oxo-dimer of hematin show a spin state of  $5/2$ , as determined by Mössbauer spectroscopy.<sup>55–58</sup> This was the value considered in the calculations performed over the hematin complex.

Molecular electrostatic potential (MEP) surfaces were drawn using the CUBEGEN utility present in GAUSSIAN 98,<sup>54</sup> applied to the optimized geometries of all molecules. These MEP isoenenergy contours were generated in the range of  $-50$  to  $50$  kcal/mol, superimposed onto a surface of constant electron density ( $0.0002$  e/ $\text{au}^3$ ), to provide a measure of the electrostatic potential at roughly the van der Waals surface of the molecule. This color-coded surface provides a measure of the overall size of the molecule, as well as the location of negative or positive electrostatic potentials. The regions of positive electrostatic potential indicate excess positive charge, leading to repulsion of the positively charged test probe, while regions of negative potential indicate areas of excess negative charge, leading to attraction of the positively charged test probe.

Three-dimensional surfaces of molecular electrostatic potential at the constant values of  $-5$  and  $-10$  kcal/mol were generated to determine the profile of the

electrostatic potential of a molecule when approaching the receptor.

Visualization of all the results was performed with Molekel 4.2.<sup>59</sup>

### Supporting information

MEPs superimposed onto total electron density and three-dimensional electrostatic potential isosurfaces at –10 and –5 kcal/mol for all compounds studied here have been presented as the article's supporting information.

### Acknowledgements

FCT (I&D No. 226/94), POCTI (QCA III), FEDER and PRAXIS XXI Recipients of PhD grant from FCT: César Portela (SFRH/BD/3036/2000).

### References and notes

- Winstanley, P. A. *Parasitol. Today* **2000**, *16*, 146–153.
- Greenwood, B. M. *Parasitol. Today* **1997**, *13*, 90–92.
- Biagini, G. A.; O'Neill, P. M.; Nzila, A.; Ward, S. A.; Bray, P. G. *Trends Parasitol.* **2003**, *19*(11), 479–487.
- Koella, J. C. *Today* **1998**, *14*, 360–364.
- Bray, P. G.; Mungthin, M.; Ridley, R. G.; Ward, S. A. *Mol. Pharm.* **1998**, *54*, 170–179.
- Wongrichanalai, C.; Pickard, A. L.; Wernsdorfer, W. H.; Meshnick, S. R. *Lancet* **2002**, *2*, 209–218.
- May, J.; Meyer, C. G. *Trends Parasitol.* **2003**, *19*(10), 432–435.
- Ginsburg, H.; Krugliak, M. *Drug Resistance Updates* **1999**, *2*, 180–187.
- Francis, S. E.; Sullivan, D. J., Jr.; Goldberg, D. E. *Annu. Rev. Microbiol.* **1997**, *51*, 97–123.
- Blauer, G.; Akkawi, M. *J. Inorg. Biochem.* **1997**, *66*, 145–152.
- Pagola, S.; Stephens, P. W.; Bohle, D. S.; Kosar, A. D.; Madsen, S. K. *Nature* **2000**, *404*, 307–310.
- Bohle, D. S.; Dinnebier, R. E.; Madsen, S. K.; Stephens, P. W. *J. Biol. Chem.* **1997**, *272*, 713–716.
- Dorn, A.; Stoffel, R.; Matile, H.; Bubendorf, A.; Ridley, R. G. *Nature* **1995**, *374*, 269–271.
- Fitch, C. D.; Chou, A. C. *Antimicrob. Agents Chemother.* **1997**, *41*, 2461–2465.
- Zhang, J.; Krugliak, M.; Ginsburg, H. *Mol. Biochem. Parasitol.* **1999**, *99*, 129–141.
- Vippagunta, S. R.; Dorn, A.; Ridley, R. G.; Vennerstrom, J. L. *Biochim. Biophys. Acta* **2000**, *1475*, 133–140.
- Moreau, S.; Perly, B.; Biguet, J. *Biochimie* **1982**, *64*, 1015–1025.
- Moreau, S.; Perly, B.; Chachaty, C.; Deleuze, C. *Biochim. Biophys. Acta* **1985**, *840*, 107–116.
- Chou, A. C.; Fitch, C. D. *J. Clin. Invest.* **1980**, *66*, 856–858.
- Orjih, A. U.; Banyal, H. S.; Chevli, R.; Fitch, C. D. *Science* **1981**, *214*, 667–669.
- Ginsburg, H.; Demel, R. A. *Biochim. Biophys. Acta* **1983**, *772*, 316–319.
- Hebbel, R. P.; Eaton, J. W. *Semin. Hematol.* **1989**, *26*, 136–149.
- Ginsburg, H.; Famin, O.; Zhang, J.; Krugliak, M. *Biochem. Pharmacol.* **1998**, *56*, 1305–1313.
- Sugioka, Y.; Suzuki, M. *Biochim. Biophys. Acta* **1991**, *1074*, 19–24.
- Chou, A. C.; Chevli, R.; Fitch, C. D. *Biochemistry* **1980**, *19*, 1543–1549.
- Egan, T. J.; Mavuso, W. W.; Ross, D. C.; Marques, H. M. *J. Inorg. Biochem.* **1997**, *68*, 137–145.
- Sullivan, D. J., Jr.; Gluzman, I. Y.; Russell, D. G.; Goldberg, D. E. *Proc. Natl. Acad. Sci. U.S.A.* **1996**, *93*, 11865–11870.
- Sullivan, D. J., Jr.; Matile, H.; Ridley, R. G.; Goldberg, D. E. *J. Biol. Chem.* **1998**, *273*, 31103–31107.
- Dorn, A.; Vippagunta, S. R.; Matile, H.; Jaquet, C.; Vennerstrom, J. L.; Ridley, R. G. *Biochem. Pharmacol.* **1998**, *55*, 727–736.
- Orjih, A. U.; Fitch, C. D. *Biochim. Biophys. Acta* **1993**, *1157*, 270–274.
- Egan, T. J.; Ross, D. C.; Adams, P. A. *FEBS Lett.* **1994**, *352*, 54–57.
- Ursos, L. M. B.; DuBay, K. F.; Roepe, P. D. *Mol. Biochem. Parasitol.* **2001**, *112*, 11–17.
- Egan, T. J.; Hempelmann, E.; Mavuso, W. W. *J. Inorg. Biochem.* **1999**, *73*, 101–107.
- Foley, M.; Tilley, L. *Pharmacol. Ther.* **1998**, *79*, 55–87.
- Hawley, S. R.; Bray, P. G.; Mungthin, M.; Atkinson, J. D.; O'Neill, P. M.; Ward, S. A. *Antimicrob. Agents Chemoter.* **1998**, *42*, 682–686.
- Egan, T. J.; Marques, H. M. *Coord. Chem. Rev.* **1999**, *190–192*, 493–517.
- Egan, T. J. *Exp. Opin. Ther. Patents* **2001**, *11*, 185–209.
- Ziegler, J.; Linck, R.; Wright, D. W. *Curr. Med. Chem.* **2001**, *8*, 171–189.
- Vippagunta, S. R.; Dorn, A.; Matile, H.; Battacharjee, A. K.; Karle, J. M.; Ellis, W. Y.; Ridley, R. G.; Vennerstrom, J. L. *J. Med. Chem.* **1999**, *42*, 4630–4639.
- De, D.; Krogstad, F. M.; Byers, L. D.; Krogstad, D. J. *J. Med. Chem.* **1998**, *41*, 4918–4926.
- Egan, T. J.; Hunter, R.; Kaschula, C. H.; Marques, H. M.; Misplon, A.; Walden, J. *J. Med. Chem.* **2000**, *43*, 283–291.
- De, D.; Krogstad, F. M.; Cogswell, F. B.; Krogstad, D. J. *Am. J. Trop. Med. Hyg.* **1996**, *55*, 579–583.
- Ridley, R. G.; Hofheinz, W.; Matile, H.; Jaquet, C.; Dorn, A. O.; Masciadri, R. O.; Jolidon, S. O.; Richter, W. F. O.; Guenzi, A. O.; Girometta, M.; Urwyler, H.; Huber, W.; Thaithong, S.; Peters, W. *Antimicrob. Agents Chemoter.* **1996**, *40*, 1846–1854.
- Battacharjee, A. K. *J. Mol. Struct. (Theochem)* **2000**, *529*, 193–201.
- Battacharjee, A. K. *J. Mol. Struct. (Theochem)* **2001**, *549*, 27–37.
- Winter, R. W.; Cornell, K. A.; Johnson, L. L.; Ignatushenko, M.; Hinrichs, D. J.; Riscoe, M. K. *Antimicrob. Agents Chemoter.* **1996**, *40*, 1408–1411.
- Winter, R. W.; Ignatushenko, M.; Ogundahunsi, O. A. T.; Cornell, K. A.; Oduola, A. M. J.; Hinrichs, D. J.; Riscoe, M. K. *Antimicrob. Agents Chemoter.* **1997**, *41*, 1449–1454.
- Ignatushenko, M.; Winter, R. W.; Bachinger, H. P.; Hinrichs, D. J.; Riscoe, M. K. *FEBS Lett.* **1997**, *409*, 67–73.
- Ignatushchenko, M. V.; Winter, R. W.; Riscoe, M. K. *Am. J. Trop. Med. Hyg.* **2000**, *62*, 77–81.
- Bennet, G. J.; Lee, H. *Phytochemistry* **1989**, *28*, 967–998.
- Mandal, S.; Das, P. C.; Joshi, P. C. *J. Indian Chem. Soc.* **1992**, *69*, 611–636.



52. Battacharjee, A. K.; Karle, J. M. *J. Med. Chem.* **1996**, *39*, 4622–4629.
53. Menezes, C. M. S.; Sant'Anna, C. M. R.; Rodrigues, C. R.; Barreiro, E. J. *J. Mol. Struct. (Theochem)* **2002**, *579*, 31–39.
54. Frisch, M. J.; Trucks, G. W.; Schlegel, H. B.; Scuseria, G. E.; Robb, M. A.; Cheeseman, J. R.; Zakrzewski, V. G.; Montgomery, J. A., Jr.; Stratmann, R. E.; Burant, J. C.; Dapprich, S.; Millam, J. M.; Daniels, A. D.; Kudin, K. N.; Strain, M. C.; Farkas, O.; Tomasi, J.; Barone, V.; Cossi, M.; Cammi, R.; Mennucci, B.; Pomelli, C.; Adamo, C.; Clifford, S.; Ochterski, J.; Petersson, G. A.; Ayala, P. Y.; Cui, Q.; Morokuma, K.; Malick, D. K.; Rabuck, A. D.; Raghavachari, K.; Foresman, J. B.; Cioslowski, J.; Ortiz, J. V.; Baboul, A. G.; Stefanov, B. B.; Liu, G.; Liashenko, A.; Piskorz, P.; Komaromi, I.; Gomperts, R.; Martin, R. L.; Fox, D. J.; Keith, T.; Al-Laham, M. A.; Peng, C. Y.; Nanayakkara, A.; Challacombe, M.; Gill, P. M. W.; Johnson, B.; Chen, W.; Wong, M. W.; Andres, J. L.; Gonzalez, C.; Head-Gordon, M.; Replogle, E. S.; Pople, J. A. GAUSSIAN 98, Revision A.9, Gaussian, Pittsburgh PA 1998.
55. Adams, P. A.; Berman, P. A. M.; Egan, T. J.; Marsh, P. J.; Silver, J. *J. Inorg. Biochem.* **1996**, *63*, 69–77.
56. Bauminger, E. R.; Akkawi, M.; Blauer, G. *Inor. Chim. Acta* **1999**, *286*, 229–232.
57. Bohle, D. S.; Debrunner, P.; Jordan, P. A.; Madsen, S. K.; Schulz, C. E. *J. Am. Chem. Soc.* **1998**, *120*, 8255–8256.
58. Adams, P. A.; Egan, T. J.; Ross, D. C.; Silver, J.; Marsh, P. J. *Biochem. J.* **1996**, *318*, 25–27.
59. Portmann, S.; Lüthi, H. P. *CHIMIA* **2000**, *54*, 766–770.